

Can amphiphile architecture directly control vesicle size?

Martin J. Greenall and Carlos M. Marques

*Institut Charles Sadron, University of Strasbourg,
CNRS - UPR 22, 23, rue du Loess, 67034 Strasbourg, France*

(Dated: July 2, 2012)

Bilayer membranes self-assembled from simple amphiphiles in solution always have a planar ground-state shape. This general principle is a robust consequence of several internal relaxation mechanisms of the membrane and prevents the straightforward control of the size of vesicles. Here, we show that this principle can be circumvented and that direct size control by molecular design is a realistic possibility. Using coarse-grained calculations, we design tetrablock copolymers that form membranes with a preferred curvature, and demonstrate how to make the free energies of these structures lower than those of other self-assembled geometries.

A fundamental process in soft matter science is the self-assembly of amphiphilic molecules into a startling variety of structures, ranging from simple micelles to complex connected aggregates [1–3]. Self-assembled structures not only occur naturally in living cells, but can also be designed for vital applications such as drug encapsulation and delivery [4]. The question that lies at the heart of this field is how the properties of the individual amphiphilic molecules control the topology of the aggregates they form [5]. One of the major unsolved problems is whether a molecule can be designed that can directly fix the curvature of a membrane in solution. In addition to its fundamental interest, this question is of great practical importance, as finding such a molecule would allow the straightforward and spontaneous formation of vesicles of a well-defined size, thereby yielding precise control of drug delivery systems.

At present, membrane curvature can only be controlled by rather complex procedures. Several of these [6–11] require two species of amphiphile to be blended [12], so that the symmetry of the inner and outer leaflets of the bilayer is broken [13] and the vesicle has a preferred radius. Such methods have the disadvantage that blends of amphiphiles can form a wide range of micellar aggregates which may coexist with the target vesicle structure [9]. Other methods involve the use of more complicated vesicle formation pathways, such as dewetting from a templated surface [14], cooling and warming through a cylinder-vesicle shape transition [15], electroformation on micropatterned glass slides [16], flow focusing in microfluidics [17], and combined extrusion and dialysis [18].

In this Letter, we investigate an alternative strategy for controlling membrane curvature. We break the membrane symmetry by the use of ABCA' tetrablock copolymers [19–21]. The outer A and A' blocks of the polymer are formed of the same hydrophilic material, and the B and C blocks are hydrophobic and have a repulsive interaction with each other. These molecules form asymmetric *monolayers* in solution [19] (see Fig. 1a), in contrast to the bilayers formed by diblocks (Fig. 1b). We use tetrablocks rather than ABC triblocks since, in this latter case, the A and C blocks would have to be hy-

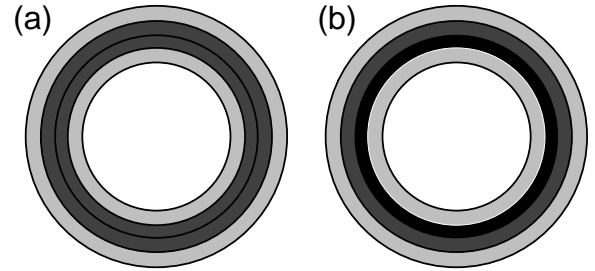


FIG. 1: (a) Bilayer vesicle formed from diblock copolymers. Hydrophilic blocks are light gray and hydrophobic blocks are dark gray. (b) Monolayer vesicle formed from tetrablock copolymers. There are now two hydrophobic blocks, colored black and dark gray respectively. The black block is more strongly hydrophobic, and segregates to the inner half of the monolayer in order to minimize the area of its interfaces with other species.

drophilic and have a strong mutual repulsion for asymmetric monolayers to form. This combination is hard to achieve, both because of the difficulty of finding hydrophilic compounds that repel strongly and the fact that the hydrophilic layers are diluted by solvent, weakening any interaction between them.

Tetrablock vesicles have indeed been formed in preliminary experimental investigations by Brannan and Bates [19], who also achieved a degree of size control of the aggregates. Such vesicles have also been found in very recent Monte Carlo simulations [21], although the question of size control was not studied. Here, we present a concrete theoretical demonstration of the basic principle that tetrablock copolymers can form bilayers of a preferred curvature, and also show how these molecules should be designed to control the vesicle radius and avoid the formation of unwanted micellar structures [20].

To capture the basic physics of the system as clearly as possible, we focus on a simple model of ABCA' tetrablocks blended with A homopolymer ‘solvent’. To begin, we consider copolymers where all four segments contain the same number of monomers $N/4$. For simplicity, the A homopolymer molecules were also taken to contain $N/4$ monomers. The strength of the interactions between the

various species are set by Flory χ parameters. We note that once two χ parameters have been chosen, the third must be calculated from a relation involving the polarizabilities of the various species [22]. To calculate the density profiles and free energies of the self-assembled structures, we used a simple coarse-grained mean-field theory (self-consistent field theory, or SCFT) in which the individual polymer molecules are modeled by random walks and their interactions by a contact potential [23, 24]. The great advantage of SCFT for our current investigation is that it is simpler and faster than, for example, Monte Carlo methods, allowing the free energy to be computed for a large range of vesicle sizes and the question of optimum bilayer curvature to be directly addressed. Furthermore, for the high molecular weight synthetic polymers considered here, SCFT can approach Monte Carlo simulations in accuracy [25] and can yield considerable qualitative insights even into aqueous solutions of these molecules [9]. The diffusion equations describing the random-walk polymers were solved by a standard finite-difference method and the SCFT equations by an iterative scheme [26].

Since we focus on curved membranes, and in particular on spherical vesicles, we perform many of our calculations assuming spherical symmetry in a spherical calculation box, although other geometries will also be considered. As these calculations involve only a single aggregate, we must make the connection between the free energy of the subsystem of volume V containing the vesicle and that of the system as a whole. To do this, we calculate the free-energy density \tilde{F} of a box containing a single spherically-symmetric vesicle in the canonical ensemble. We measure all energies in units of $k_B T$, and make \tilde{F} dimensionless by multiplication by the volume v of a single copolymer molecule. We then vary the volume of the simulation box at constant overall copolymer volume fraction [27]. In a very simple way, this mimics a larger system (of fixed total volume and fixed copolymer volume fraction) searching for its free energy minimum by varying the number of aggregates and hence the volume occupied by each. If the calculated free energy density has a minimum as a function of the volume of the calculation box, this means that the aggregates have a preferred size, and, in our case, that the vesicle membranes have an optimum curvature.

Although this minimum corresponds to the absolute free energy minimum of a solution of spherical vesicles, the shape of the curve $\tilde{F}(V)$ is not directly linked to the size distribution of the aggregates in a real system, as a point on the curve corresponds a *monodisperse* solution of vesicles of a given size. Fortunately, these results can be interrogated further to calculate the polydispersity Δ of the vesicles, which arises from fluctuations around the free energy minimum. In theories of micellization [28], this is related to the curvature of the free energy f_p of an aggregate of p molecules by $1/\Delta^2 = \partial^2 f_p / \partial p^2$. To ex-

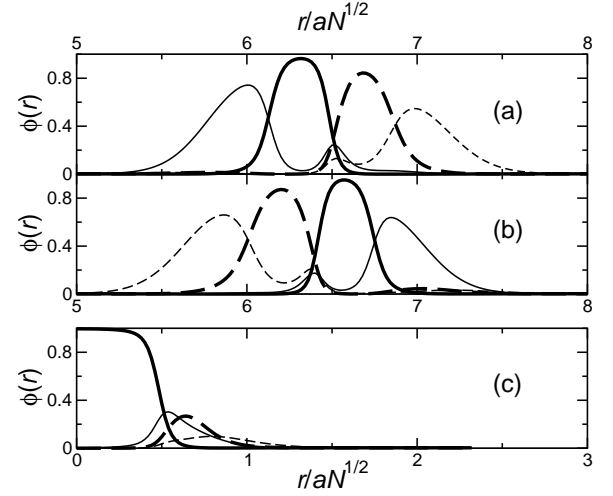


FIG. 2: Sample volume fraction profiles for (a) ABCA' vesicles, (b) vesicles in the unfavorable A'CBA orientation, and (c) micelles. A-blocks: thin full lines, B-blocks: thick full lines, C-blocks: thick dashed lines, A'-blocks: thin dashed lines.

tract this quantity from our curves of $\tilde{F}(V)$, we write the (dimensionless) free energy density of our monodisperse solution of aggregates in terms of f_p as

$$\tilde{F} = (\phi - v_m/V) \ln[(\phi - v_m/V)/e] + (\phi - v_m/V)f_1 + v f_p/V \quad (1)$$

where ϕ is the volume fraction of copolymer molecules, $1/V$ is the number density of aggregates, $v_m = pv$ is the volume of an aggregate, f_1 is the energy of an isolated copolymer in solution, and f_p is the energy of an aggregate of p copolymers. The first term arises from the entropy of the free copolymers in solution. Now, we note that a single SCFT calculation finds the local free energy minimum $\tilde{F}(V)$ for a vesicle in a box of volume V . In the process, it determines the optimum number of molecules in the vesicle for this box size and therefore corresponds to minimizing \tilde{F} with respect to p at a given $1/V$. Varying the box size then yields the curve $\tilde{F}(V)$, from which we can read off the second derivative $\partial^2 \tilde{F} / \partial V^2$. Remembering that this derivative is evaluated along the line where $\partial \tilde{F} / \partial p|_V = 0$, we find, by differentiation and rearrangement of Eq. 1, that

$$\frac{1}{\Delta^2} = \frac{\partial^2 f_p}{\partial p^2} = \frac{v}{v_m^2 / (V^3 \partial^2 \tilde{F} / \partial V^2) - (\phi V - v_m)} \quad (2)$$

allowing us to calculate Δ .

We now demonstrate the existence of the target vesicle structure as a solution to SCFT. In Fig. 2b, we plot cuts through the density profile of an ABCA' vesicle, with the overall copolymer volume fraction fixed to 0.05. The various χ parameters must be large enough for the amphiphile to aggregate, and so we set $\chi_{AB} = 50/N$ and $\chi_{AC} = 30/N$, where N is the total number of monomers

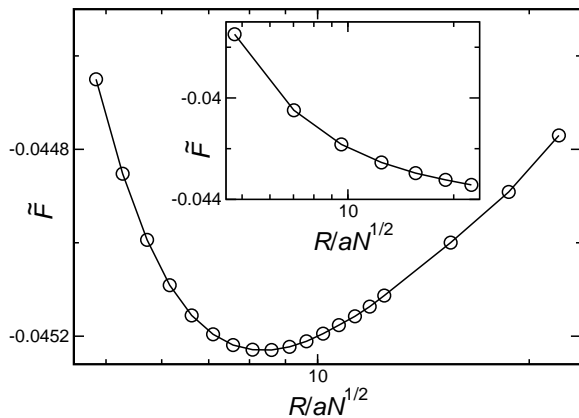


FIG. 3: Minimum of the free energy density as a function of vesicle radius R . The free energy F_h of a homogeneous system of the same composition is subtracted and the free energy density is made dimensionless by multiplication by the volume v of a single molecule. The inset shows the corresponding curve for vesicles formed of tetrablock polymers in the unfavorable A'CBA orientation.

in the copolymer. So that the B and C species demix, we choose the larger of the two possible values [22] for χ_{BC} , which we set to $157.5/N$. We measure all lengths in units of $aN^{1/2}$, where a is the segment length [24].

The ABCA' structure sketched in Fig. 1 is clearly reproduced in our calculations. The strongly hydrophobic B-blocks lie in the inner half of the membrane, so that the more energetically unfavorable AB interface has a smaller area than the A'C interface. Figure 2a shows that the local density is highest in the B layer, and lower in the more diffuse hydrophilic corona. We note also that the density profiles of both hydrophilic blocks have small peaks in the center of the vesicle wall. This is because a fraction of the copolymers fold back on themselves to protect the strongly incompatible B and C species from each other. Surprisingly, we also find solutions to SCFT, shown in Fig. 2b, where the vesicle is 'inside-out', with the B species on the outside of the vesicle core, increasing the size of the AB interface.

In Fig. 2c, we plot the density profile of a micelle, formed in a smaller calculation box. Here, the micelle core is formed from the strongly hydrophobic B blocks, while the other species mix in the corona. This structure is most likely formed as in ABA triblock micelles [29], with the copolymers forming a hairpin shape.

We now focus on the free energies of the structures plotted in Fig. 2, and in particular on their size dependence. In Fig. 3, we plot the free energy density \tilde{F} as a function of the ABCA' vesicle radius R (defined as the radius on the outside of the vesicle at which the copolymer and solvent densities are equal), which we vary by changing the calculation box size as detailed above. For concreteness, we fix the zero of our free energy scale to correspond to a homogeneously-mixed system of the

same composition. This choice does not affect our calculations of polydispersity, which require only the curvature $\partial^2 \tilde{F} / \partial V^2$. The curve shows a clear minimum as a function of R , demonstrating that the vesicles have a preferred size. This is in sharp contrast to the monotonic decrease of the free energy density of the A'CBA vesicle, plotted in the inset.

An insight into the mechanism behind the existence of an optimum vesicle size can be gained by comparison of the two curves. At smaller radii, the free energy density of both vesicles decreases with increasing size, as the chains relax and the copolymers are no longer strongly compressed on the inner face of the membrane. The ABCA' vesicle always has a lower free energy than the A'CBA vesicle, as the unfavorable AB interface is on the inside and is therefore smaller. As the vesicle radius increases, both membranes become flatter and the relative advantage of the ABCA' vesicle decreases. The two lines then start to approach each other, with the ABCA' curve now rising and the A'CBA curve continuing to fall. The monotonic form of the A'CBA curve is also clear evidence that the ABCA' minimum is not a finite size effect.

To calculate the relative polydispersity Δ/p of the vesicles, we plot the main free energy curve of Fig. 3 as a function of subsystem volume V , allowing us to calculate the curvature $\partial^2 \tilde{F} / \partial V^2$ at the minimum. We calculate the aggregate volume v_m by integrating over the vesicle density profile and subtracting the local volume fraction at the edge of the system, where it has attained a stable bulk value. To proceed further with this calculation, we estimate the volume v of a single copolymer molecule. By recalling that all volumes are measured in units of $a^3 N^{3/2}$, and defining the segment volume such that $v = a^3 N$, we can show that Δ/p is given by the product of a term specified uniquely by our SCFT calculations and $1/N^{1/4}$. This shows that the polydispersity is rather insensitive to the choice of degree of polymerization within the physically reasonable range [20] of $N \sim 100 - 1000$. Even using the smallest of these values, $N = 100$, we find clear size selection, with a relative polydispersity of $\Delta/p \approx 0.09$. Since the vesicle is relatively flat, we can assume that its surface area is proportional to p and hence that its radius is proportional to $p^{1/2}$. This yields a relative polydispersity in terms of the radius of 0.05, and shows that strong size selection can be obtained in our simple model system.

By reducing the simulation box size further, we also find a minimum in the free energy density corresponding to a spherical micelle (not shown in Fig. 3). However, for the strongly repulsive interactions studied here, this structure, in which the incompatible A and C species must mix in the corona (see Fig. 2c), has a much higher free energy density than the ABCA' vesicle, with $\tilde{F} \approx -0.034$. By performing calculations in a cylindrical box at the same copolymer volume fraction, we can also find a free-energy minimum corresponding to an (infinite) cylin-

drical micelle, which, at $\tilde{F} \approx -0.037$, lies in between those of the spherical micelle and the ABCA' vesicle. The ABCA' vesicle therefore has the lowest free energy of all simple structures for the current parameters. This situation changes if the hydrophobicity of the C-blocks is reduced so that $\chi_{AC} = 20/N$ and $\chi_{BC} = 133.2/N$. In this case, the spherical micelle has the lowest free energy density, with $\tilde{F} \approx -0.028$, since the A and C species can now mix more freely in the corona. The next lowest free energy is that of the cylindrical micelle, $\tilde{F} \approx -0.023$, while the free energy of the ABCA' vesicle is now much higher than that of the micelles, with $\tilde{F} \approx -0.0076$. Recent experiments have indeed shown that ABCA' copolymers can form micelles rather than planar structures at room temperature [20], and this result demonstrates how copolymers with sufficiently high χN might be used to avoid this outcome.

To address the important practical question of how the architecture of the copolymer affects the optimum vesicle radius, we repeat the calculation of the free energy minimum shown in Fig. 3 with the size of the B-blocks increased by 10%. This leads to a growth of the radius from $R \approx 8.4aN^{1/2}$ to $R \approx 9.4aN^{1/2}$, to avoid unfavorable compression of the longer B-blocks on the inner half of the vesicle membrane. This opens the possibility of rather fine control of the vesicle size by the degree of polymerization of the hydrophobic blocks.

In summary, we have demonstrated that the curvature of membranes in solution can be controlled by the architecture of the constituent amphiphilic molecules. Specifically, we use coarse-grained calculations to show that copolymers composed of two central hydrophobic blocks and two outer hydrophilic blocks form vesicles with a preferred radius. To our knowledge, this is the only system where the molecular structure of the amphiphiles can be shown directly to fix the curvature of a membrane in solution. Control of curvature has only been achieved before by mixing two types of amphiphile or by using a mechanically complex self-assembly method. We have also shown how to encourage the formation of vesicles by the use of appropriate block chemical nature and how to adjust the preferred radius by changing the block length.

Several practically important extensions to our research suggest themselves. Our current coarse-grained methods can be implemented in a straightforward manner to explore the chemical parameter space more comprehensively; in particular, the role of the various block lengths and interaction strengths in fixing vesicle size and polydispersity could be investigated fully. Also, the model can be strengthened by introducing further molecular details, for example using dissipative particle dynamics [30] or Monte Carlo [21], with a particular view to realistic modeling of the solvent and to optimizing the experimental polymer parameters for the production of nearly monodisperse vesicles.

-
- [1] X. He and F. Schmid, Phys. Rev. Lett. **100**, 137802 (2008).
 - [2] S. Jain and F. S. Bates, Science **300**, 460 (2003).
 - [3] L. F. Zhang and A. Eisenberg, Science **272**, 1777 (1996).
 - [4] E. Haleva and H. Diamant, Phys. Rev. Lett. **101**, 078104 (2008).
 - [5] S.-H. Choi, T. P. Lodge, and F. S. Bates, Phys. Rev. Lett. **104**, 047802 (2010).
 - [6] J. H. Lee, V. Agarwal, A. Bose, G. F. Payne, and S. R. Raghavan, Phys. Rev. Lett. **96**, 048102 (2006).
 - [7] E. W. Kaler, A. K. Murthy, B. E. Rodriguez, and J. A. N. Zasadzinski, Science **245**, 1371 (1989).
 - [8] K. Katagiri and F. Caruso, Adv. Mater. **17**, 738 (2005).
 - [9] F. Li, S. Prévost, R. Schweins, A. T. M. Marcelis, F. A. M. Leermakers, M. A. C. Stuart, and E. J. R. Sudhölter, Soft Matter **5**, 4169 (2009).
 - [10] M.-P. Nieh, T. A. Harroun, V. A. Raghunathan, C. J. Glinka, and J. Katsaras, Phys. Rev. Lett. **91**, 158105 (2003).
 - [11] R. Joannic, L. Auvray, and D. D. Lasic, Phys. Rev. Lett. **78**, 3402 (1997).
 - [12] F. Campelo and A. Hernandez-Machado, Phys. Rev. Lett. **100**, 158103 (2008).
 - [13] S. A. Safran, P. Pincus, and D. Andelman, Science **248**, 354 (1990).
 - [14] J. R. Howse, R. A. L. Jones, G. Battaglia, R. E. Ducker, G. J. Leggett, and A. J. Ryan, Nat. Mater. **8**, 507 (2009).
 - [15] A. Rank, S. Hauschild, S. Förster, and R. Schubert, Langmuir **25**, 1337 (2009).
 - [16] P. Taylor, C. Xu, P. D. I. Fletcher, and V. N. Paunov, Chem. Commun. pp. 1732–1733 (2003).
 - [17] J. Thiele, D. Steinhäuser, T. Pfohl, and S. Förster, Langmuir **26**, 6860 (2010).
 - [18] T. F. Zhu and J. W. Szostak, PLoS ONE **4**, e5009 (2009).
 - [19] A. K. Brannan and F. S. Bates, Macromolecules **37**, 8816 (2004).
 - [20] E. D. Gomez, T. J. Rappl, V. Agarwal, A. Bose, M. Schmutz, C. M. Marques, and N. P. Balsara, Macromolecules **38**, 3567 (2005).
 - [21] J. Cui and W. Jiang, Langmuir **27**, 10141 (2011).
 - [22] F. Schmid, in *Handbook of Multiphase Polymer Systems*, edited by A. Boudenne (John Wiley and Sons, Chichester, 2011), chap. 3.
 - [23] S. F. Edwards, Proc. Phys. Soc. **85**, 613 (1965).
 - [24] M. W. Matsen, in *Soft Matter*, edited by G. Gompper and M. Schick (Wiley-VCH, Weinheim, 2006), chap. 2.
 - [25] A. Cavallo, M. Müller, and K. Binder, Macromolecules **39**, 9539 (2006).
 - [26] J. U. Kim and M. W. Matsen, Phys. Rev. Lett. **102**, 078303 (2009).
 - [27] M. J. Greenall, D. M. A. Buzza, and T. C. B. McLeish, J. Chem. Phys. **131**, 034904 (2009).
 - [28] S. Puvvada and D. Blankschtein, J. Chem. Phys. **92**, 3710 (1990).
 - [29] K. Ulrich, P. Galvosas, J. Kärger, and F. Grinberg, Phys. Rev. Lett. **102**, 037801 (2009).
 - [30] P. J. Hoogerbrugge and J. M. V. A. Koelman, Europhys. Lett. **19**, 155 (1992).